

# MASSIVE PLANET MIGRATION: THEORETICAL PREDICTIONS AND COMPARISON WITH OBSERVATIONS

PHILIP J. ARMITAGE<sup>1,2</sup>

*Received 2007 March 21; accepted 2007 May 15*

## ABSTRACT

We quantify the utility of large radial velocity surveys for constraining theoretical models of type II migration and protoplanetary disk physics. We describe a theoretical model for the expected radial distribution of extrasolar planets that combines an analytic description of migration with an empirically calibrated disk model. The disk model includes viscous evolution and mass loss via photoevaporation. Comparing the predicted distribution to a uniformly selected subsample of planets from the Lick, Keck, and AAT planet search programs, we find that a simple model in which planets form in the outer disk at a uniform rate, migrate inward according to a standard type II prescription, and become stranded when the gas disk is dispersed is consistent with the radial distribution of planets for orbital radii in the range  $0.1 \text{ AU} \leq a < 2.5 \text{ AU}$  and planet masses  $M_p > 1.65 M_J$ . Some variant models are disfavored by existing data, but the significance is limited ( $\sim 95\%$ ) due to the small sample of planets suitable for statistical analysis. We show that the favored model predicts that the planetary mass function should be almost independent of orbital radius at distances where migration dominates the massive planet population. We also study how the radial distribution of planets depends on the adopted disk model. We find that the distribution can constrain not only changes in the power-law index of the disk viscosity, but also sharp jumps in the efficiency of angular momentum transport that might occur at small radii.

*Subject headings:* accretion, accretion disks — planetary systems: formation —  
 planetary systems: protoplanetary disks — planets and satellites: formation —  
 solar system: formation

## 1. INTRODUCTION

Radial velocity and transit searches for extrasolar planets have detected more than 170 low-mass companions around nearby, mostly solar-type stars (Butler et al. 2006). These detections, which result from radial velocity surveys targeting a few times  $10^3$  stars, have allowed for an initial determination of the distribution of massive extrasolar planets with mass, orbital radius, eccentricity, and stellar metallicity (Santos et al. 2004; Marcy et al. 2005; Fischer & Valenti 2005; Santos et al. 2005). The statistical (and, hopefully, systematic) errors on these determinations will improve as ongoing surveys press to larger orbital radii and smaller planet masses. Substantially larger radial velocity surveys of  $10^5$ – $10^6$  stars, with precision in the  $\sim 10 \text{ m s}^{-1}$  range, are technically possible over the next decade (Ge et al. 2006). Given this rapid observational progress, it is of interest to ask how much information about planet formation, planet migration, and the protoplanetary disk is retained in the statistical properties of extrasolar planets and could be potentially tapped via an expansion of existing planet samples. Put more bluntly, is it worth obtaining much larger samples of planets with properties similar to those already known, or does the primary scientific interest for future surveys lie in exploring entirely new regimes of parameter space?

At sufficiently small orbital radii, massive extrasolar planets very probably migrated inward from formation sites further out rather than forming in situ (Lin et al. 1996; Trilling et al. 1998; Bodenheimer et al. 2000). There remains some uncertainty in quantifying “sufficiently small,” but it seems likely that massive planet formation is most common outside the snow line (Hayashi et al. 1985). Protoplanetary disk models clearly show that the radius of the snow line changes dramatically with time as the

disk evolves (Garaud & Lin 2007), so to quote a single radius is potentially misleading. However, for a solar-type star, the apparent presence of hydrated minerals in solar system asteroids allows an empirical determination of the location of the snow line at a radius of around 2.7 AU (Morbidelli et al. 2000). This suggests that most of the extrasolar planets currently known, which orbit within a few AU of their host stars, derive their properties largely via migration. For massive planets, the appropriate regime of migration is thought theoretically to be the type II regime, which involves migration within a gap in the protoplanetary disk (Goldreich & Tremaine 1980; Lin & Papaloizou 1986), rather than the gapless type I regime appropriate to Earth-mass planets and giant planet cores (Ward 1997). Since direct observational evidence of migration is currently lacking, the only possible tests of this theory come from statistical comparison with the observed properties of extrasolar planetary systems. Indeed, prior work along these lines by Armitage et al. (2002), Trilling et al. (2002), and Ida & Lin (2004) has shown that the distribution of observed planets in orbital radius (and, in the case of the Ida & Lin [2004] study, planetary mass) is broadly consistent with theoretical expectations based on disk migration within an evolving protoplanetary disk.

In this paper, we develop more refined predictions for the radial distribution of massive planets on the basis of a simple analytic model for type II migration. Our main goal is to determine, at least in principle, what might be learned from comparisons of large planet samples with theoretical models. In § 2 we describe the adopted model for the protoplanetary disk and how migration of massive planets within the disk is treated. In § 3 we compute the predicted distribution of planets in orbital radius. We compare the predictions to the observed distribution of planets in the Fischer & Valenti (2005) sample, which has previously been used to study the dependence of planet frequency on host metallicity. This sample has a clearly specified selection limit, which allows for a reliable statistical comparison between the model and observations. In §§ 4 and 5 we investigate the extent to which migration

<sup>1</sup> JILA, University of Colorado, Boulder, CO 80309; pja@jilau1.colorado.edu.

<sup>2</sup> Department of Astrophysical and Planetary Sciences, University of Colorado, Boulder, CO 80309.

TABLE 1  
PROPERTIES OF SELF-SIMILAR DISK MODELS

Power-Law Index of Viscosity $\gamma$	Viscosity Normalization $\nu_0$	Initial Disk Mass $M_{\text{disk}}$ ( $M_\odot$ )
0.5.....	$1.52 \times 10^8 \text{ cm}^{3/2} \text{ s}^{-1}$	0.057
1.0.....	$15.62 \text{ cm s}^{-1}$	0.051
1.5.....	$1.58 \times 10^{-6} \text{ cm}^{1/2} \text{ s}^{-1}$	0.058

NOTE.—All three models meet the observational constraints on the evolution of the stellar accretion rate discussed in the text (§ 2).

leads to a radial variation in the exoplanet mass function and how sensitive it is to structure within the protoplanetary disk. These sections are primarily forward-looking, since existing data are too limited to support or refute the theoretical model. We conclude in § 6 with some discussion of the results.

## 2. TYPE II MIGRATION WITHIN THE PROTOPLANETARY DISK

We consider a model in which massive planets form within an evolving protoplanetary disk at radii beyond the snow line and migrate inward within a gap (“type II” orbital migration). Migration slows and eventually ceases as the gas disk is dispersed. We assume that photoevaporation causes disk dispersal. The resulting distribution of massive planets in orbital radius then depends on the disk model (which is reasonably tightly constrained by observations), the migration rate (which is known reasonably well theoretically), and the rate of planet formation in the disk as a function of time. The latter can in principle be predicted from a model of massive planet formation, but here we treat it as a free function.

The surface density  $\Sigma$  of a protoplanetary disk that evolves under the combined action of an effective kinematic viscosity  $\nu$  and mass loss per unit area  $\dot{\Sigma}_{\text{wind}}(r)$  is described by (Pringle 1981)

$$\frac{\partial \Sigma}{\partial t} = \frac{3}{r} \frac{\partial}{\partial r} \left[ r^{1/2} \frac{\partial}{\partial r} \left( \nu \Sigma r^{1/2} \right) \right] - \dot{\Sigma}_{\text{wind}}(r), \quad (1)$$

provided that the mass lost in the wind has the same specific angular momentum as the disk at the launch point. If we approximate the angular momentum transport in the disk as a time-independent kinematic viscosity that is a power law in radius,

$$\nu = \nu_0 r^\gamma, \quad (2)$$

equation (1) admits a compact self-similar solution if the mass-loss rate is negligible (Lynden-Bell & Pringle 1974; Hartmann et al. 1998). In this solution the surface density evolves according to

$$\Sigma(R, T) = \frac{C}{3\pi\nu_{\text{scale}} R^\gamma} T^{-(5/2-\gamma)/(2-\gamma)} \exp\left(-R^{2-\gamma}/T\right), \quad (3)$$

where the scaled variables  $R$  and  $T$  are defined via a fiducial radius  $r_{\text{scale}}$ :

$$R \equiv \frac{r}{r_{\text{scale}}}, \quad (4)$$

$$\nu_{\text{scale}} \equiv \nu(r_{\text{scale}}), \quad (5)$$

$$T \equiv \frac{t}{t_{\text{scale}}} + 1, \quad (6)$$

$$t_{\text{scale}} = \frac{1}{3(2-\gamma)^2} \frac{r_{\text{scale}}^2}{\nu_{\text{scale}}}. \quad (7)$$

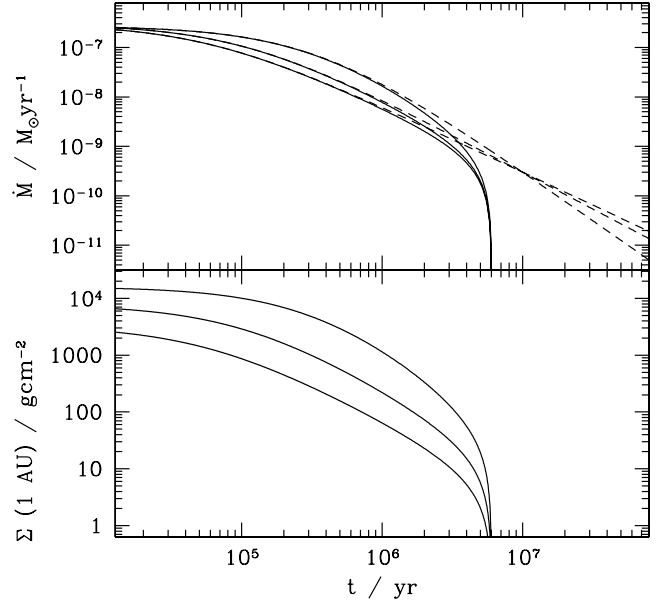


FIG. 1.—Time dependence of the accretion rate onto the central star, plotted for different disk models. The three dashed curves in the top panel show the predicted evolution in self-similar models with different power-law exponents for the disk viscosity:  $\gamma = 0.5$ ,  $\gamma = 1.0$ , and  $\gamma = 1.5$ . The solid curves show the result including photoevaporation, which is here modeled using the solution of Ruden (2004), assuming a disk dispersal time of 6 Myr. The analytic cutoff is derived assuming  $\gamma = 1.0$ , but it should be a good approximation for general power-law viscosity profiles. The bottom panel shows the surface density evolution at a disk radius of 1 AU (the  $\gamma = 1.5$  model is the uppermost curve).

The constant  $C$  is the mass accretion rate at  $t = 0$  as  $r \rightarrow 0$ . Other quantities, such as the mass accretion rate  $\dot{M}$  and the radial velocity  $v_r$  in the disk, can be derived straightforwardly using these expressions.

We constrain the parameters of the similarity solution (eq. [3]) to be consistent with the observational analysis of the time dependence of T Tauri accretion rates presented by Muzerolle et al. (2000). We fix all models to have an initial accretion rate  $\dot{M}(t = 0) = 3 \times 10^{-7} M_\odot \text{ yr}^{-1}$ , which decays to  $\dot{M} = 3 \times 10^{-10} M_\odot \text{ yr}^{-1}$  in  $10^7$  yr if the disk lives that long before being dispersed. We also fix  $r_{\text{scale}} = 10$  AU. Table 1 shows the values of the viscosity normalization constant  $\nu_0$  and the initial disk mass  $M_{\text{disk}}$  that meet these constraints for different values of the power-law index  $\gamma$ . Not surprisingly, since the basic observational constraints have been known for some time, the disk models that we favor have parameters similar to those considered in many previous studies (Hartmann et al. 1998; Armitage et al. 2003; Alexander et al. 2006). Figure 1 shows the resulting evolution of the accretion rate for these models.

The power-law decline in the late-time accretion rate implied by the similarity solution does not yield the sharp transition between accreting classical T Tauri stars and nonaccreting weak-lined T Tauri stars that is observed (Simon & Prato 1995; Wolk & Walter 1996). It is plausible that this transition is driven by photoevaporation (Bally & Scoville 1982) from the outer disk, which acts to starve the inner disk (thereby allowing it to drain viscously onto the star on a short timescale) once the accretion rate becomes comparable to the wind mass-loss rate (Clarke et al. 2001). If photoevaporation is driven by irradiation from the central star, then the simplest analytic models predict that the mass-loss rate per unit area scales as (Hollenbach et al. 1994)

$$\dot{\Sigma}_{\text{wind}} \propto r^{-5/2} \quad (8)$$

exterior to some critical radius  $r_{\text{in}}$ , with zero mass loss from smaller radii. The critical radius is given to an order of magnitude by the radius where the sound speed in photoionized gas ( $T \simeq 10^4$ ) first exceeds the local escape speed. This is a few AU for a solar mass star. The normalization of the mass-loss rate depends on the square root of the ionizing flux  $\Phi$ , which is hard to measure accurately but whose value can be constrained observationally (Alexander et al. 2005; Pascucci et al. 2007). Much more detailed numerical models of photoevaporation are now available (Font et al. 2004; Alexander et al. 2006), but the additional complexity they involve is not warranted for this application. Accordingly, we assume a time-independent mass-loss rate of the form given by equation (8), with  $r_{\text{in}} = 5$  AU, and zero mass loss at smaller radii.

Once photoevaporation is included (in this simplified form), it is still possible to derive a Green's function solution to equation (1) (Ruden 2004), but there is no compact form for the evolution of  $\Sigma(r, t)$  analogous to equation (3). At late times (i.e., after the disk has evolved for several viscous times) and small radii ( $r < r_{\text{in}}$ ), however, it is possible to derive an expression for the reduction in the inner accretion rate and surface density caused by the wind. Defining  $t_0$  as the time at which the inner accretion rate falls to zero as a consequence of the mass loss from the outer disk, Ruden (2004) finds that the time dependence of the accretion rate at small radii is as follows:

$$\dot{M} = \left[ 1 - \left( \frac{t}{t_0} \right)^{3/2} \right] \dot{M}_{\text{ss}}, \quad (9)$$

where  $\dot{M}_{\text{ss}}$  is the accretion rate evolution predicted by the self-similar model in the absence of any mass loss. The suppression of accretion implied by the term in brackets is derived for  $\gamma = 1$ , but it should also be approximately valid for other values of the power-law viscosity index. Using numerical solutions to equation (1), we have verified that the Ruden (2004) formula provides a good description of the evolution of the accretion rate and inner surface density during the transition, and hence we apply the same cutoff to generate the surface density evolution including wind loss  $\Sigma(r, t)$  from the self-similar prediction (eq. [3]). On the basis of observations of disk frequency in young clusters (Haisch et al. 2001), we take  $t_0 = 6$  Myr, which yields the accretion rate evolution shown by the solid curves in Figure 1. As has been emphasized previously (Clarke et al. 2001; Armitage et al. 2003), to a good approximation, the disk evolution proceeds as if there is no mass loss while  $\dot{M} \gg \dot{M}_{\text{wind}}$  and is then dispersed rapidly once mass loss becomes significant. Figure 1 also shows the evolution of the inner (1 AU) disk surface density. Irrespective of the value of  $\gamma$ , all of the disk models considered have an *initial* surface density that is substantially in excess of the minimum mass solar nebula reference value (Weidenschilling 1977), but this drops rapidly as the disk evolves. By the time that massive planets migrate through this region (after several Myr of evolution), the surface density has fallen by at least an order of magnitude. The import of this is that the local disk mass during migration is typically smaller than the mass of giant planets, a regime that leads to a significantly slower inspiral.

Sufficiently massive planets are able to open a gap within the gaseous protoplanetary disk and, having opened a gap, migrate inward<sup>3</sup> in lockstep with the gas via type II migration (Lin &

Papaloizou 1986). For a planet at orbital radius  $r_p$ , the gravitational torques exerted by the planet on the surrounding disk are strong enough to maintain a gap provided that the mass ratio  $q = M_p/M_*$  satisfies (Takeuchi et al. 1996)

$$q \gtrsim \left( \frac{c_s}{r_p \Omega_p} \right)^2 \alpha^{1/2}, \quad (10)$$

where  $c_s$  and  $\Omega_p$  are the sound speed and the angular velocity in the disk at the radius of the planet, respectively, and  $\alpha$  is the dimensionless Shakura-Sunyaev viscosity parameter (Shakura & Sunyaev 1973). Noting that the thickness of the disk  $h \simeq c_s/\Omega_p$ , we find that the  $\gamma = 1$  disk model specified in Table 1 would correspond to an equivalent value of  $\alpha \simeq 5 \times 10^{-3}$  (matching the viscosity at 5 AU around a solar mass star, assuming that the disk has  $h/r = 0.05$ ). The viscous gap-opening criteria is then satisfied for planets with masses exceeding about  $0.2 M_J$ . The thermal gap-opening condition is satisfied at a similar mass (Bate et al. 2003). In this paper, we exclusively consider planets with masses of  $1 M_J$  and above, which should accordingly be safely in the gap-opening regime of parameter space.

To compute the type II migration rate within the disk model specified above, we draw on the results of Syer & Clarke (1995). These authors noted that the rate of migration, which is sometimes assumed to equal the radial velocity that gas in the disk *would have in the absence of a planet*, is suppressed once the planet mass exceeds a local estimate of the disk mass. Specifically, they defined a measure of the importance of the disk relative to the planet,

$$B \equiv \frac{4\pi\Sigma r_p^2}{M_p}, \quad (11)$$

that is small if the planet dominates the angular momentum budget of the planet + disk system and large otherwise. The type II migration rate is then given for  $B \geq 1$  (the disk-dominated case) by

$$\dot{r}_p = v_r, \quad (12)$$

while for  $B < 1$  (the planet-dominated limit),

$$\dot{r}_p = B^{1/2} v_r, \quad (13)$$

where we have assumed (consistent with eq. [2]) that the efficiency of angular momentum transport is independent of the surface density. For our disk models, Figure 2 shows the critical accretion rate below which  $B < 1$  for a Jupiter-mass planet. In all these models, the slowdown of the migration rate occurs due to the inertia of the planet for accretion rates substantially greater than those at which photoevaporation starts to influence the disk evolution. The effect on the nominal migration timescale,

$$t_{\text{mig}} \equiv \frac{r_p}{|\dot{r}_p|}, \quad (14)$$

is shown in Figure 3. The  $B < 1$  limit is applicable at all radii of interest in a disk with  $\dot{M} = 10^{-10} M_\odot \text{ yr}^{-1}$ , and within radii less than a few AU (depending on the planet mass) in a disk with  $\dot{M} = 10^{-8} M_\odot \text{ yr}^{-1}$ .

Once planets exceed the critical gap-opening mass by a significant factor, the rate of accretion onto the planet across the

<sup>3</sup> Here we consider exclusively planets that form close enough in that the sense of gas flow and migration is inward; planets that form further out may instead absorb the angular momentum of the inner disk and move outward (Veras & Armitage 2004; Martin et al. 2007) or become stranded outside the annular hole that is predicted to form as photoevaporation proceeds (Clarke et al. 2001; Matsuyama et al. 2003).

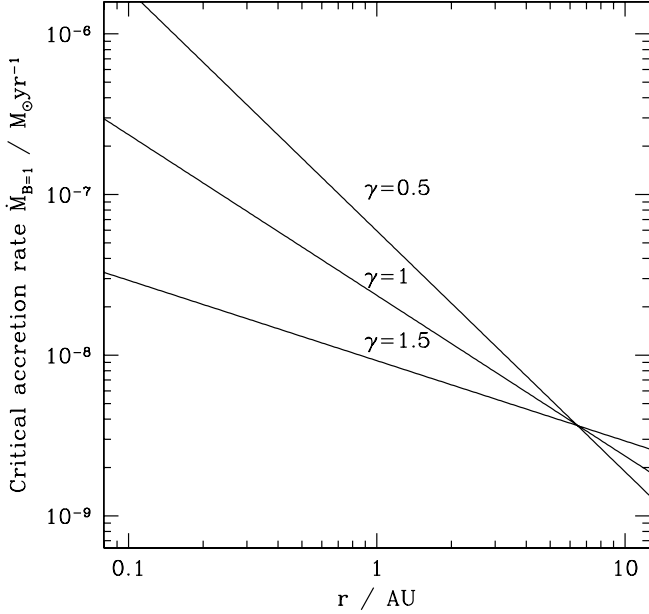


FIG. 2.—Critical accretion rate above which a  $1 M_J$  planet migrates as a test particle, plotted as a function of radius for the different disk models.

gap drops rapidly (Lubow et al. 1999). Our goal is to compare theoretical predictions for the planet distribution with a complete subsample of extrasolar planets, which requires a cut at approximately  $1.5 M_J$ . Most of the planets that survive this cut have masses substantially greater than the gap-opening mass, so *as a first approximation* it seems reasonable to ignore the possibility of mass accretion during type II migration and assume that negligible mass is accreted across the range of radii (interior to 2.5 AU) over which we make the comparison. The results of Bate et al. (2003), which show that planets can grow rapidly to masses beyond that of Jupiter while suffering little migration, support this approximation. It is then easy, using equations (12) and (13), to calculate the final (following disk dispersal) orbital radius of a planet that forms with mass  $M_p$  at radius  $a_{\text{form}}$  and time  $t_{\text{form}}$  in one of the disk models specified in Table 1. The resulting mapping between the formation conditions and the final state is the basic input needed to make a prediction of the resulting planet distribution.

The above model represents our attempt to define a “best-guess” description of type II migration within the protoplanetary disk. One may note that in the planet-dominated  $B < 1$  limit, the predicted rate of type II migration is reduced by the square root of  $B$  rather than the full ratio of the local disk mass to the planet mass. We refer to this as *partial suppression* of the migration rate. The rate is not fully suppressed because gas accumulates close to the tidal barrier as the disk + planet system evolves, increasing the torque beyond the value that would occur in an unperturbed disk (Pringle 1991). In practice, however, some gas may overflow the gap to be either accreted by the planet or to flow into an inner disk interior to the gap (Lubow & D’Angelo 2006). With this in mind, we have also computed models in which the migration rate in the planet-dominated regime is *fully suppressed*, such that

$$\dot{r}_p = Bv_r. \quad (15)$$

The difference between the partially and fully suppressed calculations provides an indication as to how sensitive the results are to uncertainties in the treatment of massive planet migration.

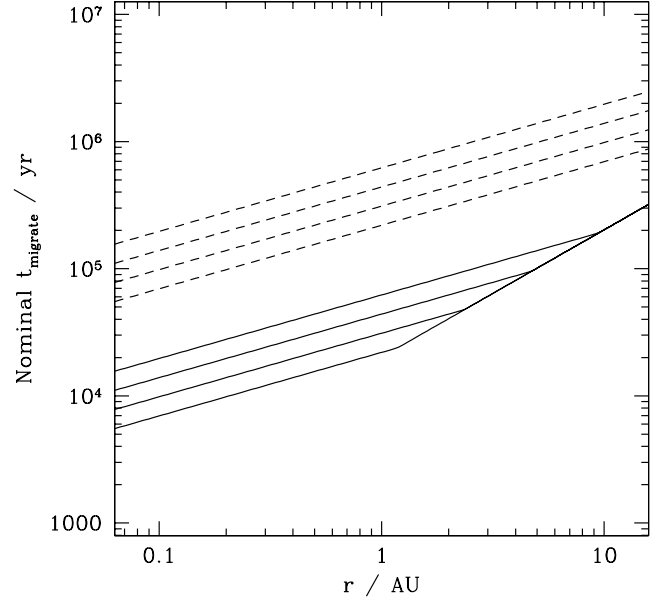


FIG. 3.—Predicted migration timescale as a function of radius in the  $\gamma = 1$  disk model. The solid lines show the migration timescale for planets of masses  $0.5 M_J$ ,  $1 M_J$ ,  $2 M_J$ , and  $4 M_J$  when the disk accretion rate is  $10^{-8} M_{\odot} \text{yr}^{-1}$  (more massive planets have longer migration timescales at small orbital radii). The dashed lines show results for planets of the same masses in a disk with  $\dot{M} = 10^{-10} M_{\odot} \text{yr}^{-1}$ .

### 3. PREDICTED DISTRIBUTION OF PLANETS IN ORBITAL RADIUS

Using the analytic disk evolution and migration models described in § 2, we compute the radius  $a_{\text{final}}$  at which massive planets become stranded as a function of the time  $t_{\text{form}}$  at which they form within the protoplanetary disk. The parameters of the model are the planet mass, the power-law index of the disk viscosity, the formation radius, and whether the migration rate is partially or fully suppressed. Illustrative results for a formation radius of 5 AU and a planet mass of  $1 M_J$  are shown in Figure 4. As is well known, planets that form at earlier epochs migrate to smaller final radii, and as the orbital radii decrease, the window of allowed formation times also narrows (Trilling et al. 2002; Armitage et al. 2002). For the favored model, in which migration is only partially suppressed, all surviving planets must form during the last 1–1.5 Myr of the disk lifetime. This is not so short a window as to imply that the planet formation process must be worryingly lossy, but it does imply that the final masses of giant planets might well reflect details of the disk dispersal process (Shu et al. 1993). Planets can form and survive across a larger fraction of the disk lifetime if instead migration is fully suppressed. There are also significant differences in the outcome that depend on the adopted disk model. These arise because of the differing profiles of the radial velocity as a function of radius, but they are less significant than the differences in the treatment of migration.

To translate these results into a prediction for the orbital distribution of massive planets, we note that

$$\frac{dN_p}{da} = \frac{dt_{\text{form}}}{da_{\text{final}}} \frac{dN_p}{dt_{\text{form}}}, \quad (16)$$

where  $dN_p/dt_{\text{form}}$  is the rate at which planets of a given mass form in the outer disk. The simplest assumption is that this rate is a constant, or at least can be approximated as such, over the interval of time near the end of the disk lifetime during which

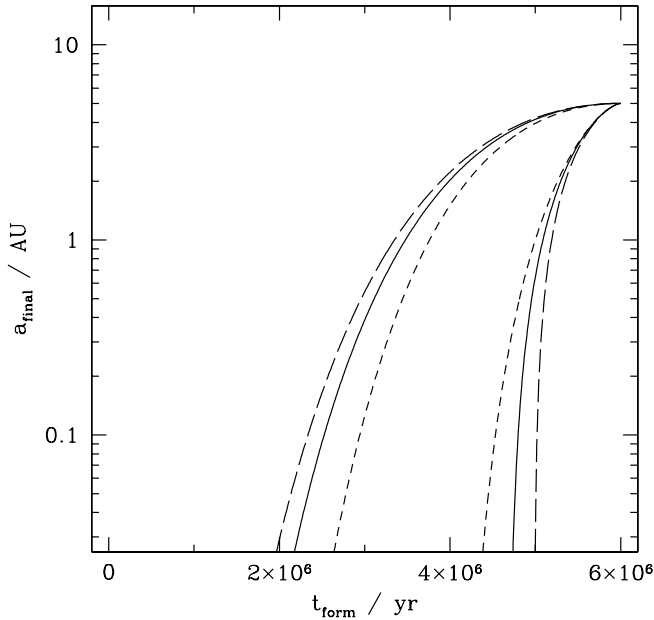


FIG. 4.—Predicted final radii for  $1 M_J$  planets as a function of the time at which they formed at 5 AU in the protoplanetary disk. The three closely spaced curves on the right-hand side of the figure show results for disks with  $\gamma = 0.5$  (long-dashed lines),  $\gamma = 1$  (solid lines), and  $\gamma = 1.5$  (short-dashed lines), assuming that migration is suppressed at small radii according to the Syer & Clarke (1995) model. The left-hand curves show the results if, instead, migration is fully suppressed by the ratio of the local disk mass to the planet mass. Differences between migration treatments are evidently more significant than differences between the disk models. For the favored models in which migration is partially suppressed, the survival time of planets in the disk is in the range of 10%–20% of the disk lifetime.

planets can form and survive migration without being swept into the star. Making this assumption, we compute and plot in Figure 5 the values of  $dN_p/d \log a$  for a variety of models that differ in the assumed formation radius, disk model, and migration treatment. Numerical values for three of these models, which assume  $a_{\text{form}} = 5$  AU, partial suppression of the migration velocity, and either  $\gamma = 0.5$ ,  $\gamma = 1$ , or  $\gamma = 1.5$ , are tabulated in Table 2. These three cases roughly bracket the range of predicted outcomes for all of the models that we have considered.

Although all of the curves have the same general form—relatively few planets are predicted to be stranded at very small orbital radii, with the number increasingly rapidly as  $a$  increases—there are significant differences that may in principle leave signatures in the observed distribution of extrasolar planets. Most importantly, the predicted number of planets per logarithmic interval in semimajor axis rises sharply as the formation radius is approached. A model in which planets are assumed to form typically at 10 AU rather than 5 AU results in a much smaller predicted number of planets at 4 AU, whereas assuming a typical formation radius of 3 AU (i.e., immediately outside the snow line) leads to a predicted pileup of planets as that radius is approached. Observational detection of a rapid increase in the number of planets at a particular orbital radius would then be a signature of a preferred orbital radius for giant planet formation. Also easily detectable are the differences between the partially and fully suppressed migration models. If migration is fully suppressed, then the number of planets (expressed as  $dN_p/d \log a$ ) at 0.1 AU is predicted to be around half the number at 1 AU, whereas for partial suppression this ratio is around 0.25. This result is easily understood: differences in the treatment of migration are most

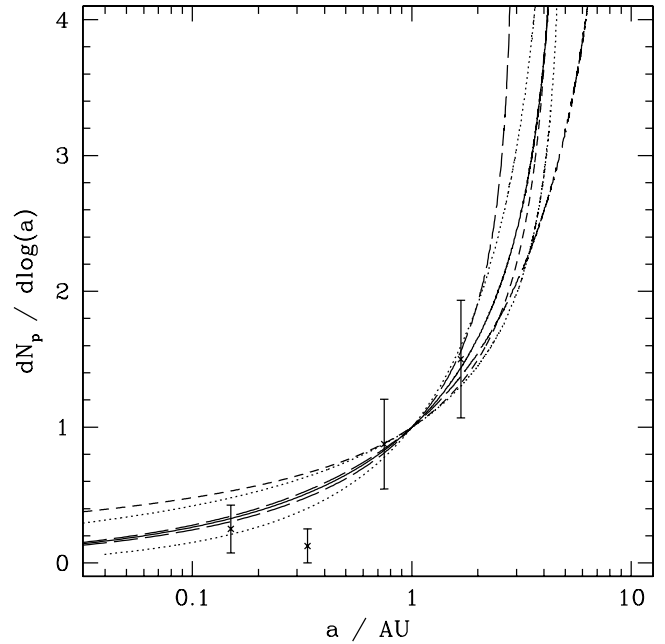


FIG. 5.—Predicted distribution of massive planets as a function of radius. All the curves show results for Jupiter-mass planets (note that the mass dependence is sufficiently weak that essentially identical results apply also for higher masses). The solid curve shows the results for the favored model, in which planets form at 5 AU at a constant rate in a  $\gamma = 1$  disk and migration is partially suppressed at small radii. The two dotted curves show the effect of varying the disk viscosity to  $\gamma = 0.5$  or  $\gamma = 1.5$ . The long-dashed curves show the effect of assuming that planets form at 3 AU (the curve furthest to the left at 2.5 AU) or 10 AU rather than at 5 AU. The short-dashed curve is the predicted distribution in the case in which migration is fully suppressed. The data points (shown with approximate errors) show the number of observed extrasolar planets with  $1.65 M_J < M_p \sin i < 10 M_J$  in a uniform and complete sample of planets constructed from that of Fischer & Valenti (2005).

TABLE 2  
PREDICTED NUMBER OF PLANETS PER LOGARITHMIC INTERVAL IN SEMIMAJOR  
AXIS FOR MODELS IN WHICH PLANET FORMATION OCCURS AT 5 AU  
AND THE MIGRATION RATE IS PARTIALLY SUPPRESSED

$\log(a/\text{AU})$	$dN(\gamma = 0.5)/d \log a$	$dN(\gamma = 1.0)/d \log a$	$dN(\gamma = 1.5)/d \log a$
−1.0	0.152	0.263	0.420
−0.9	0.184	0.298	0.423
−0.8	0.221	0.338	0.489
−0.7	0.266	0.384	0.529
−0.6	0.320	0.436	0.573
−0.5	0.385	0.497	0.623
−0.4	0.463	0.567	0.679
−0.3	0.559	0.650	0.743
−0.2	0.676	0.747	0.816
−0.1	0.820	0.863	0.899
0.0	1.000	1.000	1.000
0.1	1.226	1.170	1.117
0.2	1.518	1.380	1.261
0.3	1.912	1.656	1.448
0.4	2.458	2.035	1.705
0.5	3.283	2.592	2.080

NOTES.—Results for three different values of  $\gamma$  are quoted. These results approximately bracket the shallowest to steepest curves obtained for the models shown in Fig. 5. Results are quoted for  $1 M_J$  planets, but the mass dependence is weak, much weaker than the differences between the models with different values of  $\gamma$ . The numbers have been normalized to unity at 1 AU.

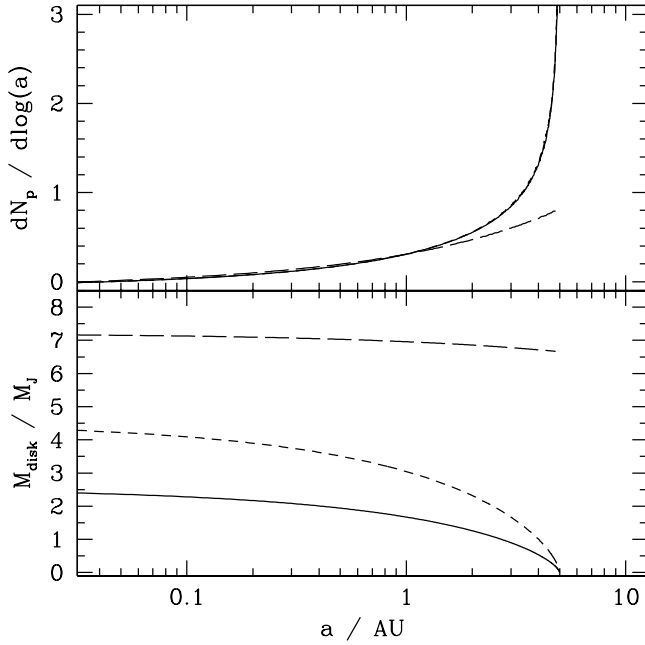


FIG. 6.—Predicted distribution of massive planets as a function of radius (*top*), plotted together with the disk mass evaluated at the formation epoch (*bottom*). The solid curve shows the results for the favored model, in which planets form at 5 AU at a constant rate in a  $\gamma = 1$  disk and migration is partially suppressed at small radii. The short-dashed curve, which is almost indistinguishable from the solid curve in the top panel, shows the effect of reducing the disk dispersal time  $t_0$  from 6 Myr to 3 Myr. The long-dashed curve shows the results of assuming an instantaneous dispersal of the disk at 6 Myr.

important at those small radii, interior to 1 AU, where the disk mass is lowest.

### 3.1. Sensitivity to the Disk Dispersal Mechanism

Our parameterization of disk evolution sweeps much that is poorly known about photoevaporation into a single parameter: the disk dispersal time  $t_0$ . Physically, rapid dispersal (small values of  $t_0$  for a given set of disk initial conditions) will occur for large values of the ionizing flux  $\Phi$ , which will drive a stronger photoevaporative flow. Quantitatively, the total mass-loss rate from the disk scales as (Hollenbach et al. 1994)

$$\dot{M}_{\text{wind}} \simeq 1.5 \times 10^{-10} \left( \frac{\Phi}{10^{41} \text{ s}} \right)^{1/2} \left( \frac{M_*}{M_\odot} \right)^{1/2} M_\odot \text{ yr}^{-1}, \quad (17)$$

where the prefactor has been adjusted from the analytic value to better match the numerical results of Font et al. (2004) and the fiducial ionizing flux has been chosen to be consistent with observational estimates (Alexander et al. 2005; Pascucci et al. 2007), which are, however, subject to substantial uncertainties.

With our disk models, a wind mass-loss rate in the range between  $10^{-10}$  and  $10^{-9} M_\odot \text{ yr}^{-1}$  yields the dispersal time of 6 Myr that is our baseline assumption. Our fiducial parameters are therefore consistent with standard photoevaporation models. A consequence of this, however, is that the *disk mass* at the epoch when surviving planets form is quite small. Figure 6 shows the gas disk mass at the moment planets form as a function of the final planet semimajor axis. For the models we have considered, the typical disk masses are only a few Jupiter masses if migration is partially suppressed (in the fully suppressed case, on the other hand, surviving planets form substantially earlier, when there is plenty of disk gas remaining). These small masses directly reflect the efficiency of the migration process: relatively modest

amounts of gas are able to drive substantial migration. However, they do pose a possible consistency problem: planets that form in very low mass disks evidently perturb the disk structure substantially, and this might affect the final planetary distribution.

To explore this possibility, we considered two options. First, within the formalism developed here, we have investigated the effect of reducing  $t_0$  so that surviving planets form earlier when the disk mass is higher. As shown in Figure 6, a model computed with  $t_0 = 3$  Myr yields an almost identical planet distribution. Second, we have compared the results for  $\gamma = 1.5$  with the numerical models presented in Armitage et al. (2002). In the numerical models, planet masses are restricted to be no larger than a local estimate of the disk mass, and the feedback of a massive planet on the structure of a very low mass disk is explicitly followed. Reasonably good agreement is obtained between the numerical and analytic schemes, with the magnitude of the differences being comparable to the differences between the curves plotted in Figure 5.

A related question is how important the nature of the disk dispersal mechanism is for the resulting planet distribution. Physically, a model in which there is *no* mass loss from the disk exterior to the planet (either via a wind, or via accretion onto the planet) fails to yield any surviving planets; ultimately, the disk, no matter how small, absorbs the orbital angular momentum of the planet and drives it to small radius.<sup>4</sup> However, many other models in which the disk is dispersed rapidly do yield sensible distributions, so it is of interest to assess how sensitive the planet distribution is to the specifics of disk dispersal. To gauge this, we have considered an extreme model in which the disk evolves viscously for 6 Myr without any mass loss and is then instantaneously dispersed. Figure 6 depicts the resulting planet distribution. At small radii (within about 1.5 AU) this model tracks the fiducial photoevaporative case closely, but further out, the instantaneous dispersal model yields a much flatter distribution. This reflects the fact that in the case of photoevaporation, the migration of the last planets to form is limited by the rapid drop in the disk surface density, and these planets pile up at radii relatively close to their formation sites. We conclude that the innermost part of the extrasolar planet distribution (within roughly an AU) ought to be largely independent of how the disk is dispersed, but that the distribution further out does depend on whether photoevaporation or some other mechanism is at work.

### 3.2. Effect of the Dispersion in Disk Properties

The disk models used in this paper have been adjusted to approximately reproduce the mean lifetimes and accretion rates of observed disks (Haisch et al. 2001; Hartmann et al. 1998). This procedure ignores the fact that, observationally, there is a large dispersion in the accretion rate at a given age. This dispersion exceeds that expected from measurement uncertainties in accretion rates and stellar ages.

The origin of the intrinsic dispersion in disk properties as a function of system age is not known, and hence it is impossible to make a blanket statement as to whether consideration of a mean model is reasonable or not. We can, however, distinguish some possibilities. One possibility (Armitage et al. 2003) is that the dispersion in disk properties arises from a dispersion in disk initial conditions (disk mass, disk angular momentum). Since the planet distribution depends only on the disk evolution close

<sup>4</sup> Strictly speaking, this is only true if the inner disk is subject to a zero-torque boundary condition. A steady state solution is possible if there is instead angular momentum injection at small radii; for example, due to the interaction between the disk and the stellar magnetosphere (Armitage & Clarke 1996).

to the transition epoch (independent of the absolute timing), in this scenario the ensemble distribution averaged over the population would be expected to be the same as the mean model we have computed. Of course, giant planet formation would be less probable in short-lived disks with low initial surface densities (Pollack et al. 1996), so in practice most planets would form in those disks with higher initial surface densities at radii of a few AU.

A second possibility is that the observed dispersion in accretion rates arises from changes in individual accretion rates on timescales intermediate between the disk lifetime and observable timescales. Apart from thermal instabilities (Bell & Lin 1994), which are only likely to be relevant for initial accretion rates higher than those we have considered here, no obvious candidate instabilities that might yield large fluctuations in  $\dot{M}$  are known, but it remains possible that  $\dot{M}(r)$  might vary rapidly. If such variability extended across the radial range considered here, it is likely that the migration history of planets would be altered.

### 3.3. Comparison with a Uniformly Selected Data Set

We compare the models to a subsample of extrasolar planets detected by the Keck, Lick, and AAT planet search programs. Initially, we proceed rather conservatively and define a subsample that is as complete and unbiased as possible over specified intervals in planet mass and orbital radii. Our procedure is as follows:

1. We start with a sample of 850 stars of FGK spectral types targeted by the Lick, Keck, and AAT planet search programs for which 10 or more radial velocity measurements over a period of at least 4 yr are available. This sample is listed in Table 3 of Fischer & Valenti (2005). For these stars, hypothetical planets that yield a radial velocity semi-amplitude of  $K > 30 \text{ m s}^{-1}$  have nearly uniform detectability, provided that the orbital period is less than 4 yr. The orbital period restriction corresponds to a maximum semimajor axis of 2.5 AU, assuming solar mass hosts. From this sample, Fischer & Valenti (2005) list 46 stars that host known extrasolar planets. In some cases, these are multiple systems.

2. In many cases, additional radial velocity data are available beyond those used by Fischer & Valenti (2005). We therefore update the orbital elements quoted by Fischer & Valenti (2005) to match those reported by Butler et al. (2006). Typically the changes to the derived masses and semimajor axes are rather modest (here we ignore eccentricity, which in some cases is more substantially altered). Including the multiple planets in some systems, this yields a sample of 59 planets.

3. Finally, we define a subsample that includes only planets that are massive enough to be detectable across the entire range of orbital radii for which the survey is complete. At 2.5 AU,  $K = 30 \text{ m s}^{-1}$  corresponds to a planet mass of  $1.65 M_J$ , so we discard planets with smaller masses. We also cut the sample at the high-mass end, somewhat arbitrarily, at  $10 M_J$ . In terms of radial extent, we include those planets with  $0.1 \text{ AU} < a < 2.5 \text{ AU}$ . This excludes planets with very tight orbits whose dynamics may have been influenced by tidal effects and/or penetration into the protostellar magnetosphere.

It is somewhat striking, given the large number of extrasolar planets now known, how little of the publicly available data can be used for the sort of statistical comparison we are attempting here. Demanding both completeness (which restricts the stellar sample used) and lack of mass bias (which restricts the minimum mass) leaves us with only 22 massive planets. Obviously this small sample size limits the statistical power to constrain theoretical models. However, the sample should be free of any

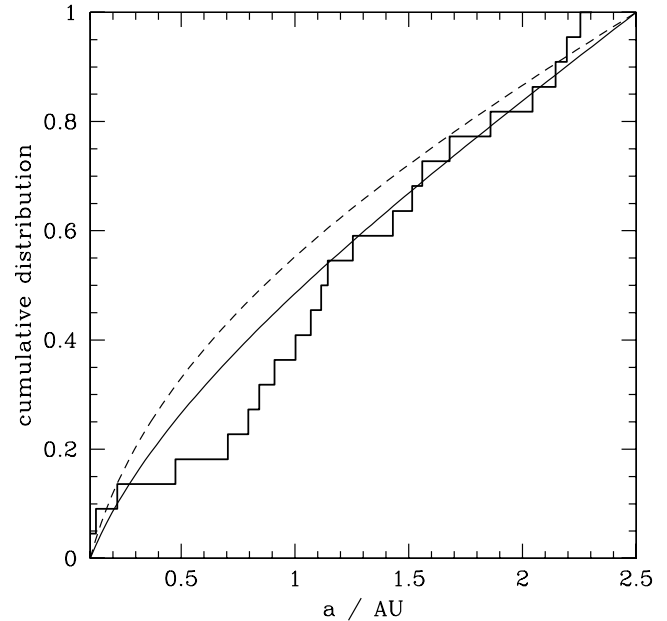


FIG. 7.—Comparison of the predicted planet distribution with the observed one. The solid histogram shows the cumulative radial distribution of massive planets with  $M_p \sin i > 1.65 M_J$ . The sample is based on that of Fischer & Valenti (2005), with the planet properties updated using the compilation of Butler et al. (2006). The solid curve shows the prediction of the fiducial model for planets of mass  $3 M_J$  formed at 5 AU in a disk with  $\gamma = 1$  and partial suppression of the migration velocity. The dashed curve shows the predictions of a model in which  $\gamma = 1.5$  but all other parameters remain fixed. This model, and other alternate models that predict flatter distributions, are not supported by the data, although the distributions cannot be distinguished at much better than the 95% confidence level.

systematic biases, which may not have been true for earlier analyses that typically used larger compilations of detected planets. For illustrative purposes, we divide the planets in our subsample into four logarithmic bins in semimajor axis (between 0.1 and 2.5 AU) and plot the number of planets in each bin over the theoretical curves in Figure 5. The observed distribution, in agreement with the theoretical models, rises rapidly with increasing semimajor axis.

Figure 7 shows the cumulative distribution of orbital radii for massive planets in the sample, together with selected theoretical curves derived from the differential distributions plotted in Figure 5. The baseline model, in which planets form at a constant rate at relatively small orbital radii (5 AU) in a protoplanetary disk with  $\gamma = 1$ , is shown as the solid curve. This model is consistent with the available data (a Kolmogorov-Smirnov test yields  $P = 0.3$ ). Of the variant models considered, those in which migration is fully suppressed,  $\gamma > 1$ , or planets are considered to typically form at larger radii are disfavored, as these models predict relatively more planets at sub-AU orbital radii than are observed. A model in which  $\gamma = 1.5$ , with the other parameters remaining unchanged, is shown as the dashed curve. This model is disfavored at modest statistical significance ( $P = 0.06$ ). Several variant models that we have considered are disfavored at roughly comparable confidence levels (95%), but with such a small observed sample, few definitive conclusions can be drawn.

As noted above, our sample selection procedure is deliberately conservative. We have also compared the theoretical model to a larger sample, obtained by taking the entire catalog of extrasolar planets from Butler et al. (2006) and retaining those planets with orbital radii in the range  $0.1 \text{ AU} < a < 2.5 \text{ AU}$  and masses in the range  $1.65 M_J < M_p \sin i < 10 M_J$  (i.e., the same mass and radius cuts as before, but relaxing the condition that all planets

were detected from one survey with well-known selection properties). The resulting sample of 53 planets has a radial distribution that, by eye, looks very similar to the 22 planet sample, and the greater numbers give us more power to discriminate between models. The baseline model ( $\gamma = 1$ , formation at 5 AU, partially suppressed migration) remains consistent with the data, while the second model discussed above, in which  $\gamma = 1.5$ , is more clearly inconsistent ( $P = 3 \times 10^{-3}$ ). We do not place much weight on these results, since the compilation of planets reported in Butler et al. (2006) is not uniformly selected. However, they illustrate clearly that only modest expansion of the sample size—by around a factor of 2—would allow us (within the formal confines of the model) to test whether the observed distribution of massive extrasolar planets is or is not consistent with theoretical models that differ in their assumptions as to planet formation radius, migration rate, and disk properties. Since some of these parameters are partially degenerate, somewhat larger unbiased samples would be needed to pin down empirically a single favored model.

#### 4. RADIAL VARIATION OF THE MASS FUNCTION

At small orbital radii where  $B < 1$ , the migration velocity is dependent on the planet mass. In the case in which migration is partially suppressed,  $\dot{r}_p \propto M_p^{-1/2}$ , and hence the fraction of time over which the most massive planets ( $10M_J$ ) can form and survive without migrating into the star is a factor of a few greater than that for Jupiter-mass planets. In a steady state disk, however, the fractional suppression of the migration velocity as a function of radius is fixed for each planet mass (at radii where  $B < 1$ ). Hence, it is approximately true that the *relative* number of planets left stranded at different radii is independent of the planet mass, and the predicted mass function of giant planets is independent of radius (Armitage et al. 2002).

In more detail, however, migration does lead to some fractionation of the planet mass function. More massive planets must form earlier than their less massive counterparts if they are to end up at the same orbital radii after disk dispersal, and the evolution of the disk is itself time-dependent (dominated by viscous evolution early on, with a change to a steeper decline in the mass accretion rate later on due to the influence of photoevaporation). To quantify the extent to which this results in a radial variation of the mass function, we assume that at small orbital radii the mass function can be written as a power law,

$$\frac{dN_p}{dM_p} \propto M_p^{-\alpha}, \quad (18)$$

and compute the predicted radial variation in  $\alpha$ . Figure 8 shows the results for two of the models that we have discussed earlier, including the baseline model. For definiteness, we set  $\alpha = 1$  at small radii, although this choice is arbitrary. The predicted variation in the mass function with orbital radius in these models is nonzero, but in these and other similar models we have computed in which the migration properties of low- and high-mass planets are the same, the magnitude of the change is small: on the order of  $\Delta\alpha = 0.1$  or less. It is straightforward to show that variations of this magnitude are undetectable with feasible surveys. The conclusion is that any detectable change in the mass function with radius (at small orbital radii where migration rather than mass growth is the dominant effect) would have to be attributed to causes other than mass-dependent migration.

There is one exception to this rule. If the migration *regime* for high-mass planets is different from that for low-mass planets, then large changes in the mass function with radius result. Such a change in migration regime is conceivable; for example, it is

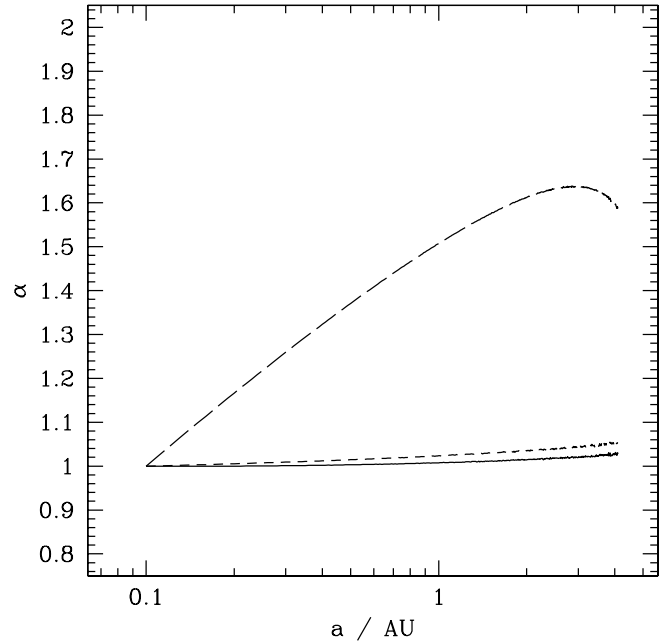


FIG. 8.—Magnitude of the predicted variation in the extrasolar planet mass function with radius in different models. The solid curve shows results from the fiducial model, in which planets form at 5 AU,  $\gamma = 1$ , and the migration velocity is partially suppressed. The short-dashed curve shows results for  $\gamma = 1.5$ , with the remaining model parameters unchanged from their fiducial values. The long-dashed curve shows the effect of assuming that a change of migration regime occurs between high- and low-mass planets. In all cases, the slope of the mass function at small radii has been fixed at  $\alpha = 1$ .

possible that high-mass planets completely prevent mass flow across the gap, while low-mass planets allow significant mass flow (Lubow et al. 1999). In this case, one would expect less perturbation to the disk structure immediately outside the gap for low-mass planets than for high-mass planets. If less mass piles up outside the tidal barrier, the torque will be reduced, and the migration velocity will go down. An example model of this kind, in which we assume that migration is fully suppressed for  $0.5 M_J$  planets but only partially suppressed for  $2 M_J$  planets, is also plotted in Figure 8. As expected (given the substantial difference between the relevant curves in Fig. 5), this model displays order-of-unity variations in the predicted slope of the mass function with radius.

Observationally, an apparent paucity of high-mass planets among the hot Jupiters has been noted by several authors (Zucker & Mazeh 2002). These planets have presumably undergone interactions with their host stars (possibly including tidal circularization, mass loss, or stopping of migration due to entry into the stellar magnetosphere), any one of which could result in either mass loss or a mass dependence to the planet's survival probability. At larger radii, however, there is no strong evidence for any variation in the mass function (Marcy et al. 2005). To illustrate this with current data, we consider the entire sample of known extrasolar planets (Butler et al. 2006) with masses in the range  $1.65 M_J < M_p \sin i < 10 M_J$  and orbital radii in the range  $0.1 \text{ AU} < a < 2.5 \text{ AU}$  (similar conclusions follow from analyses of smaller, more strictly selected samples). We divide this sample into “inner” and “outer” subsets, with equal numbers of planets in each. The dividing line between the subsets falls at a semimajor axis of 1.185 AU. Figure 9 shows the cumulative distributions of  $M_p \sin i$  for these subsamples. By eye, and statistically, no significant differences are seen. This is consistent with the predictions of the simple migration model we have developed

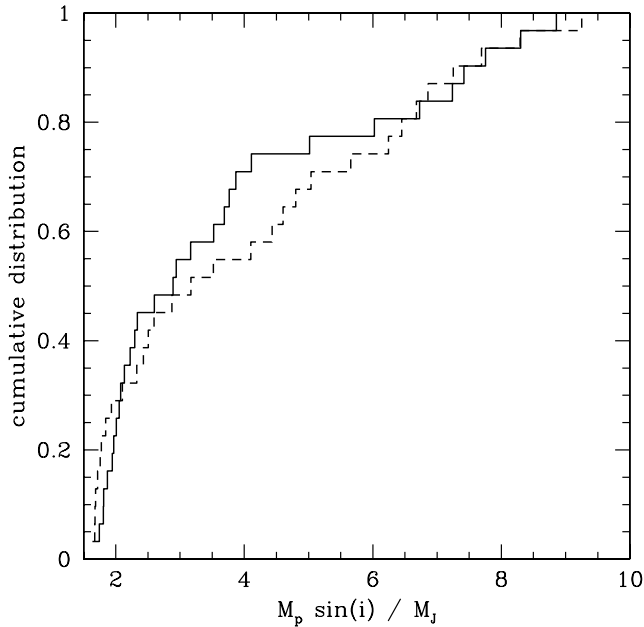


FIG. 9.—Cumulative mass function of known extrasolar planets in the mass range  $1.65 M_J < M_p \sin i < 10 M_J$ , plotted for two intervals in semimajor axis. The solid histogram shows the distribution for planets with  $0.1 \text{ AU} < a < 1.185 \text{ AU}$ , while the dashed histogram represents the distribution for planets with  $1.185 \text{ AU} < a < 2.5 \text{ AU}$ . These distributions are not statistically distinguishable.

here, and it probably already rules out the large changes in the mass function with radius predicted in the case where high- and low-mass planets migrate in a qualitatively distinct manner.

### 5. SENSITIVITY TO STRUCTURE IN THE PROTOPLANETARY DISK

The structure of the protoplanetary disk at radii on the order of 1 AU is uncertain theoretically, primarily as a consequence of the low ionization fraction, which sows doubt as to the efficiency of angular momentum transport driven by the magnetorotational instability (Balbus & Hawley 1998; Gammie 1996; Turner et al. 2007). Moreover, most existing observational constraints are either explicitly (Wilner et al. 2000) or implicitly (Hartmann et al. 1998; Armitage et al. 2003) sensitive only to large radii in the disk. Not only is the slope of the steady state surface density profile at small radii ( $\Sigma \propto r^{-\gamma}$ ) poorly known, but there could in principle be discontinuities in  $\Sigma$  due to abrupt changes in the angular momentum transport efficiency (Gammie 1996). We have looked at how both of these possibilities affect the resulting distribution of planets.

Holding other parameters of the model (primarily the planet formation radius) fixed, we plotted the resulting differential distributions of massive planets for different values of  $\gamma$  in Figure 5. Here we have assumed a smooth surface density profile, fully characterized by the value of  $\gamma$ , which we vary between  $\gamma = 0.5$  and  $\gamma = 1.5$ . The differences between these models at sub-AU radii are quite significant. If we consider the relative number of planets at 1 and 0.1 AU, the ratio varies from 2.4 ( $\gamma = 1.5$ ) to 3.8 ( $\gamma = 1$ ) to 6.6 ( $\gamma = 0.5$ ). The unbiased subsample defined earlier includes only a handful of planets at sub-AU radii, so comparison with existing data is not possible, but these differences are large enough that only a small unbiased sample of planets at these small radii would be needed to see variations of this magnitude. Changing the assumed planet formation radius has only a small influence on the distribution at sub-AU scales,

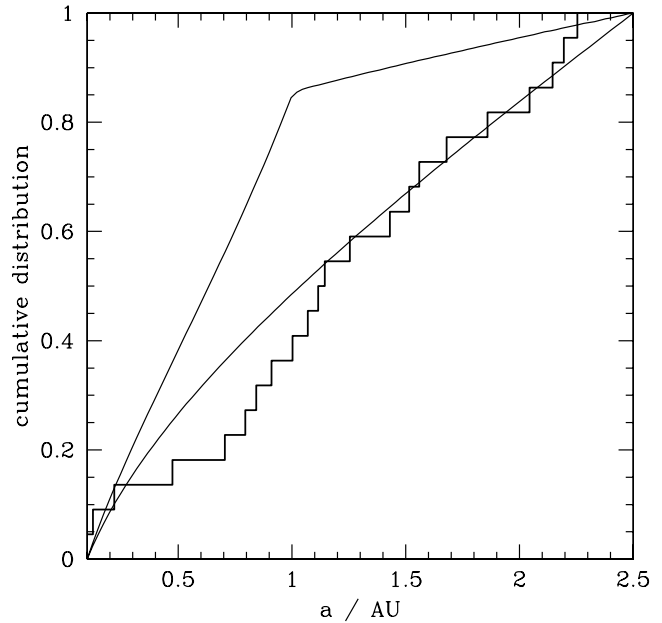


FIG. 10.—Illustration of the effect of discontinuities in the efficiency of disk angular momentum transport on the predicted planet distribution. In this not very realistic example, the viscosity is assumed to drop by a factor of 10 inside 1 AU (upper curve), leading to a large accumulation of planets at small orbital radii. As in Fig. 7, the histogram shows the observed planet distribution, and the lower curve shows the prediction of the fiducial migration model.

so the influence of different values of  $\gamma$  is in principle separable from other unknown parameters of the model.

Abrupt changes in the surface density profile—for example, due to opacity transitions within the disk or rapid changes in the efficiency of angular momentum transport with radius—leave an even more distinctive fingerprint in the radial distribution of planets, provided only that migration is not fully suppressed, so that  $\dot{r}_p$  is not linear in  $B$ . Such changes lead to a jump in the differential distribution of planets at the radius where the discontinuity occurs and correspond to a change of slope in the cumulative distribution. As an example, Figure 10 shows the predicted cumulative distribution if the viscosity is assumed to drop by a factor of 10 within 1 AU. Only rather unrealistic toy models of this kind (in which the jump is both large and situated squarely in the middle of the accessible radial range) can be ruled out using existing data, but larger data sets could potentially constrain discontinuities in the disk physics quite well.

### 6. CONCLUSIONS

In this paper we have investigated the predictions of a rather simple, almost entirely analytic model of giant planet formation and migration for the radial distribution of massive extrasolar planets. Our main results are as follows:

1. The distribution of massive planets with radius, inside the snow line beyond which planets are assumed to form, preserves information about the typical location of planet formation and the structure of the protoplanetary disk at small radii. Statistical analyses of large, uniformly selected samples of massive planets could therefore in principle be used to recover information about planet formation and disk physics.

2. Abrupt changes in the disk properties with radius, which may occur at small orbital radii, leave the most distinctive signature in the resulting planet distribution (a corresponding discontinuity in  $dN_p/d \log a$ ). Constraints on smooth surface density

profiles at AU scales are also possible, but would likely be harder to obtain and more ambiguous.

3. The mass function of extrasolar planets is not predicted to vary detectably with radius as a consequence of migration, at least in the simplest models.

4. Existing data remain compatible with a surprisingly simple model proposed previously (Armitage et al. 2002), in which massive planets form beyond the snow line at a constant rate and migrate inward through a smooth protoplanetary disk before becoming stranded when the gas disk is dispersed due to photo-evaporation. However, the sample of planets suitable for a statistical comparison with the theory is limited, and as a result a wide class of alternative models remain viable or can only be ruled out with limited significance.

Without a doubt, the simple theoretical model that we have explored here is too simple. On a technical level, it would be desirable to extend the model to properly treat the case in which planets form within a disk whose mass is only a small multiple of the planet mass, as this situation is a common outcome of the scenarios we favor. The model also ignores some effects, such as mass flow across the gap and accretion onto the planet, that are almost certainly important (Lubow et al. 1999; Lubow & D'Angelo 2006), along with others, such as planet-planet scat-

tering, which has the side effect of altering the orbital elements of surviving planets (Ford et al. 2001), that could be significant. As such, the current agreement between our predictions and the observed distribution of extrasolar planets speaks more to the paucity of the data than to the validity of the theoretical model. Taking a broader view, however, the effects that we have ignored do not appear to be so intractable that they could not, in the future, be quantified and incorporated into a theoretical model of migration. Our results therefore imply that comparison of theoretical models to the larger samples of extrasolar planets that are forthcoming holds substantial promise for learning new information about both planet formation and protoplanetary disk physics that is currently unavailable via other methods.

I thank Richard Alexander for a detailed critique of an early version of this paper, and in particular for alerting me to the work of Ruden (2004). I am also grateful to the referee for an insightful report. This work was supported by NASA under grants NAG5-13207, NNG04GL01G, and NNX07AH08G from the Origins of Solar Systems and Astrophysics Theory Programs, and by the NSF under grant AST 0407040.

#### REFERENCES

- Alexander, R. D., Clarke, C. J., & Pringle, J. E. 2005, *MNRAS*, 358, 283  
 ———. 2006, *MNRAS*, 369, 229  
 Armitage, P. J., & Clarke, C. J. 1996, *MNRAS*, 280, 458  
 Armitage, P. J., Clarke, C. J., & Palla, F. 2003, *MNRAS*, 342, 1139  
 Armitage, P. J., Livio, M., Lubow, S. H., & Pringle, J. E. 2002, *MNRAS*, 334, 248  
 Balbus, S. A., & Hawley, J. F. 1998, *Rev. Mod. Phys.*, 70, 1  
 Bally, J., & Scoville, N. Z. 1982, *ApJ*, 255, 497  
 Bate, M. R., Lubow, S. H., Ogilvie, G. I., & Miller, K. A. 2003, *MNRAS*, 341, 213  
 Bell, K. R., & Lin, D. N. C. 1994, *ApJ*, 427, 987  
 Bodenheimer, P., Hubickyj, O., & Lissauer, J. J. 2000, *Icarus*, 143, 2  
 Butler, R. P., et al. 2006, *ApJ*, 646, 505  
 Clarke, C. J., Gendrin, A., & Sotomayor, M. 2001, *MNRAS*, 328, 485  
 Fischer, D. A., & Valenti, J. 2005, *ApJ*, 622, 1102  
 Font, A. S., McCarthy, I. G., Johnstone, D., & Ballantyne, D. R. 2004, *ApJ*, 607, 890  
 Ford, E. B., Havlickova, M., & Rasio, F. A. 2001, *Icarus*, 150, 303  
 Gammie, C. F. 1996, *ApJ*, 457, 355  
 Garaud, P., & Lin, D. N. C. 2007, *ApJ*, 654, 606  
 Ge, J., et al. 2006, *Proc. SPIE*, 6269, No. 75  
 Goldreich, P., & Tremaine, S. 1980, *ApJ*, 241, 425  
 Haisch, K. E., Lada, E. A., & Lada, C. J. 2001, *ApJ*, 553, L153  
 Hartmann, L., Calvet, N., Gullbring, E., & D'Alessio, P. 1998, *ApJ*, 495, 385  
 Hayashi, C., Nakazawa, K., & Nakagawa, Y. 1985, in *Protostars and Planets II*, ed. D. C. Black & M. S. Mathews (Tucson: Univ. Arizona Press), 1100  
 Hollenbach, D., Johnstone, D., Lizano, S., & Shu, F. 1994, *ApJ*, 428, 654  
 Ida, S., & Lin, D. N. C. 2004, *ApJ*, 616, 567  
 Lin, D. N. C., Bodenheimer, P., & Richardson, D. C. 1996, *Nature*, 380, 606  
 Lin, D. N. C., & Papaloizou, J. 1986, *ApJ*, 309, 846  
 Lubow, S. H., & D'Angelo, G. 2006, *ApJ*, 641, 526  
 Lubow, S. H., Seibert, M., & Artymowicz, P. 1999, *ApJ*, 526, 1001  
 Lynden-Bell, D., & Pringle, J. E. 1974, *MNRAS*, 168, 603  
 Marcy, G., Butler, R. P., Fischer, D., Vogt, S., Wright, J. T., Tinney, C. G., & Jones, H. R. A. 2005, *Prog. Theor. Phys. Suppl.*, 158, 24  
 Martin, R. G., Lubow, S. H., Pringle, J. A., & Wyatt, M. C. 2007, *MNRAS*, 378, 1589  
 Matsuyama, I., Johnstone, D., & Murray, N. 2003, *ApJ*, 585, L143  
 Morbidelli, A., Chambers, J., Lunine, J. I., Petit, J. M., Robert, F., Valsecchi, G. B., & Cyr, K. E. 2000, *Meteoritics Planet. Sci.*, 35, 1309  
 Muzerolle, J., Calvet, N., Briceño, C., Hartmann, L., & Hillenbrand, L. 2000, *ApJ*, 535, L47  
 Pascucci, I., et al. 2007, *ApJ*, 663, 383  
 Pollack, J. B., Hubickyj, O., Bodenheimer, P., Lissauer, J. J., Podolak, M., & Greenzweig, Y. 1996, *Icarus*, 124, 62  
 Pringle, J. E. 1981, *ARA&A*, 19, 137  
 ———. 1991, *MNRAS*, 248, 754  
 Ruden, S. P. 2004, *ApJ*, 605, 880  
 Santos, N. C., Benz, W., & Mayor, M. 2005, *Science*, 310, 251  
 Santos, N. C., Israelian, G., & Mayor, M. 2004, *A&A*, 415, 1153  
 Shakura, N. I., & Sunyaev, R. A. 1973, *A&A*, 24, 337  
 Shu, F. H., Johnstone, D., & Hollenbach, D. 1993, *Icarus*, 106, 92  
 Simon, M., & Prato, L. 1995, *ApJ*, 450, 824  
 Syer, D., & Clarke, C. J. 1995, *MNRAS*, 277, 758  
 Takeuchi, T., Miyama, S. M., & Lin, D. N. C. 1996, *ApJ*, 460, 832  
 Trilling, D. E., Benz, W., Guillot, T., Lunine, J. I., Hubbard, W. B., & Burrows, A. 1998, *ApJ*, 500, 428  
 Trilling, D. E., Lunine, J. I., & Benz, W. 2002, *A&A*, 394, 241  
 Turner, N. J., Sano, T., & Dziourkevitch, N. 2007, *ApJ*, 659, 729  
 Veras, D., & Armitage, P. J. 2004, *MNRAS*, 347, 613  
 Ward, W. R. 1997, *Icarus*, 126, 261  
 Weidenschilling, S. J. 1977, *Ap&SS*, 51, 153  
 Wilner, D. J., Ho, P. T. P., Kastner, J. H., & Rodríguez, L. F. 2000, *ApJ*, 534, L101  
 Wolk, S. J., & Walter, F. M. 1996, *AJ*, 111, 2066  
 Zucker, S., & Mazeh, T. 2002, *ApJ*, 568, L113